Effects of cationic head group structure on cytotoxicity and mitochondrial actions of amphiphilic ionic liquids

Ritik Roy, Edward York, Ethan Pacchini and Tristan Rawling*

School of Mathematical and Physical Sciences, Faculty of Science, University of Technology Sydney, Sydney, NSW, 2007, Australia.

*Correspondence: Dr Tristan Rawling, School of Mathematical and Physical Sciences,

Faculty of Science, University of Technology Sydney, Ultimo, NSW

2007, Australia. Tel: (61-2)-9514-7956, Email:

Tristan.Rawling@uts.edu.au

Abstract

Ionic liquids (ILs) are a class of low melting point salts with physicochemical properties that make them suitable for a range of industrial applications. Accumulating evidence suggests that certain ILs are cytotoxic and potential environmental pollutants, thus understanding the structural features that promote IL cytotoxicity is important. Amphiphilic ionic liquids (AmILs), a class of ILs with lipophilic *N*-alkyl chains, containing aromatic head groups are generally more cytotoxic than their aliphatic counterparts, however the impact of other head group properties are less clear. This study therefore sought to provide new structure activity relationship (SAR) insights regarding the role of the cationic head group on AmIL cytotoxicity. A series of AmILs bearing a range of structurally diverse aromatic cations varying in size, charge, and lipophilicity were synthesised and screened against human MDA-MB-231 breast cancer cells. It was found that larger and more lipophilic head group increased cytotoxicity, although the magnitude of the changes were modest. The mitochondrial effects of representative ILs were assessed. The AmILs induced mitochondrial dysfunction in MDA-MB-231 cells at cytotoxic concentrations, suggesting that they target mitochondria. The new SAR information from this study may assist in the design of AmILs with controlled cytotoxicity.

Keywords: Ionic liquid; Amphiphilic cationic head group; structure-activity relationship; cytotoxicity; mitochondria.

1. Introduction

Ionic liquids (ILs) are a class of low melting point ionic compounds that are composed of bulky organic cations and inorganic anions.[1] ILs are generally stable, non-volatile and non-flammable liquids and have unique physicochemical properties that can be tuned through various cation/anion pairings to produce task-specific ILs. These properties have allowed for the development of ILs with potential applications in chemical synthesis, catalysis, battery design, biomass conversion, fuel processing, and many other fields.[2,3] Furthermore, the low volatility of ILs limits their capacity to cause atmospheric pollution, which supports the use of ILs as "green" alternatives to conventional solvents.[4] While ILs possess many features that make them attractive for use in industrial processes, there is an accumulating body of evidence showing that ILs are toxic towards plants, invertebrates, marine organisms, and mammalian cells.[5-8] This is particularly true for amphiphilic ILs (AmILs), which contain cations substituted with long *N*-alkyl chains. Given their high aqueous solubility and chemical stability, there is a risk that cytotoxic ILs could become significant environmental pollutants similar to perfluoroalkyl substances (PFASs).[9] On the other hand, the cytotoxicity of ILs suggests that these compounds may have use as antimicrobial or anticancer agents.[1,10] For example, ILs have shown to reduce the viability of a variety of cancer cells including breast (MCF-7, MDA-MB-231), cervical (HeLa), colorectal (HT-29, CaCo-2), leukaemia (HL-60), lung (A549), and liver (Hep-G2) cell lines.[11-16] ILs have also been shown to exhibit antimicrobial activity against pathogenic microorganisms including *E. coli*, *S. aureus*, *S. epidermidis*, *B. cereus*, *C. albicans*, *P. vulgaris*, *S. typhimurium*, *K. pneumonia* and *C. krusei*.[10,17,18]

It is therefore important to understand the structural features of ILs that promote toxicity, and several structure activity relationships (SAR) insights have emerged (see **Figure 1**). The length of the *N*-alkyl chain substituted on the cationic head group has been consistently shown to be the major determinant of cytotoxicity, whereby longer chain length leads to greater

3

cytotoxicity.[1,6-8,10,13-15,19-21] For example, increasing the *N*-alkyl chain of [C$_4$Py][Br] by six carbons to [C$_{10}$Py][Br] results with an ~ 150-fold increase in cytotoxicity against HeLa cells.[15] Additional studies have shown that substitution of the *N*-alkyl chain with polar functional groups (ether, nitrile, hydroxyl) lowers cytotoxicity.[22,23] The structure of the cationic head group also impacts cytotoxicity, although to a lesser extent than the *N*-alkyl chain. Several studies have shown that AmILs with aromatic head groups are more cytotoxic than non-aromatic/aliphatic ILs.[15,22,24-26] For example, Kumar *et al.*[24] found that the 1-methylpiperidinium-based AmIL [C$_8$MPip][Br] was approximately 60-fold less cytotoxic towards MCF-7 cells than the pyridinium-based AmIL [C$_8$Py][Br]. There is also some evidence to suggest that size of the cationic head group can affect IL cytotoxicity, with one report showing that AmILs with relatively larger head groups are more toxic towards HeLa cells.[16] In contrast, the nature of the anion does not appear to have a significant impact with the possible exception of the bis(trifluoromethylsulfonyl)imide (NTf$_2$) anion.[13,14] For example, butyl-substituted methylimidazolium-based ILs containing chloride, acetate, and tetrafluoroborate (BF$_4$) anions kill A2780 human ovarian adenocarcinoma cells with IC$_{50}$ concentrations between 101.6 and 123.6 μM, whereas the IC$_{50}$ of the corresponding AmIL with a NTf$_2$ anion was 12.2 μM.[13]

Anion → Minimal impact on activity
NTf$_2$ anion may increase activity

Head group
Aromatic head groups increase activity
Larger size increases activity

***N*-alkyl chain**
Major regulator of IL cytotoxicity
Chain length extension increases activity
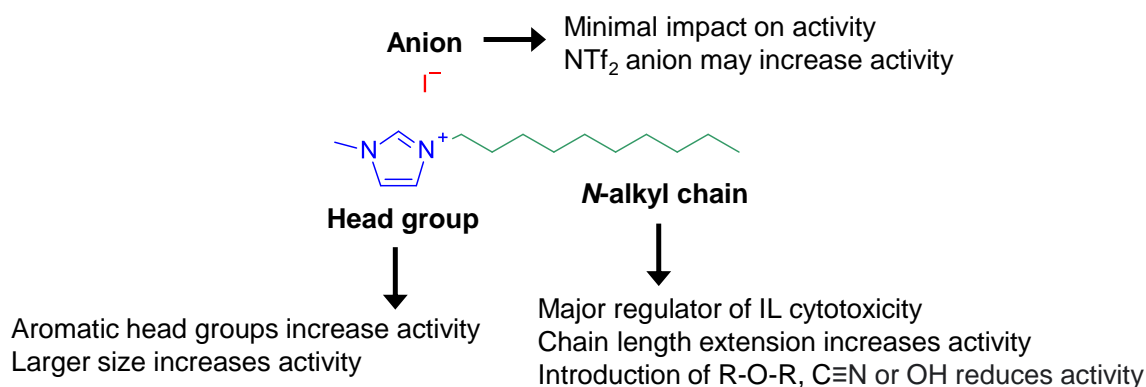Introduction of R-O-R, C≡N or OH reduces activity

Figure 1. Summary of the structure activity relationship governing IL cytotoxicity. The AmIL [C$_{10}$MiM][I] is shown as a representative chemical structure of the IL, with constituent parts highlighted in red (anion), blue (cationic head group), and green (*N*-alkyl chain).

The current SAR regarding IL cytotoxicity is limited by the low structural diversity of ILs employed in cytotoxicity studies, which focus on common head groups such as imidazolium, pyridinium and ammonium cations. Thus, the aim of this work was to expand the SAR by synthesising a series of AmILs bearing structurally diverse aromatic cationic head groups and evaluating their cytotoxicity against human MDA-MB-231 breast cancer cells. We also examined the capacity of two AmILs to permeabilise lipid membranes and induce mitochondrial dysfunction, as these have been linked to the mechanism by which AmILs exert their cytotoxic actions.[15,19,37-39] It is anticipated that the new SAR information provided by this study may assist in the design of ILs with cytotoxicity tailored for industrial and/or therapeutic applications.

2. Methods

2.1 Materials

1-Methylimidazole, 1-iodohexadecane, Dulbecco's Modified Eagle Medium (DMEM), penicillin and streptomycin, phosphate-buffered saline (PBS), DMSO, and all biochemicals and anhydrous solvents were purchased from Sigma-Aldrich (Castle Hill, NSW, Australia) and used as is. All remaining reagents were purchased from Fluorochem (Hadfield, Derbyshire, United Kingdom) and used as is. Fetal bovine serum (FBS) and trypsin/EDTA were purchased from Invitrogen, Life Technologies (Mulgrave, Victoria, Australia). 2-Dioleoyl-*sn*-glycero-3-phosphocholine (DOPC) was purchased from Avanti Polar Lipids Inc. (Alabaster, Alabama, USA).

2.2 Synthesis

Synthetic procedures and characterisation data for **1-14** are detailed in the Supporting Information. Purity of all test compounds was confirmed to be >95% by absolute quantitative NMR analysis, as previously described by Pauli *et al.*[27] This technique determines purity by calculating the proportionality between ^{1}H NMR signals against an internal reference calibrant (see Supporting Information).

2.3 Cell culture

Human MDA-MB-231 breast cancer cells were obtained from American Type Culture Collection (Manassas, Virginia, USA). MDA-MB-231 cells were grown in a humidified atmosphere of 5% CO_2 at 37 °C in DMEM supplemented with 10% FBS and 1% penicillin/streptomycin. Confluent cells (80-90%) were harvested with trypsin/EDTA after washing with PBS.

2.4 Tethered bilayer lipid membrane (tBLM) experiments

Tethered lipid bilayers were anchored across a gold electrode with 'T10' architecture, consisting of 10% benzyl-disulfide (tetra-ethylene glycol) n = 2 C_{20}-phytanyl interspacing "tethers" with 90% benzyl-disulfide-tetra-ethylene-glycol-OH "spacer" molecules.[28] Spacer and tether molecules were coordinated onto a 2.1 mm^2 gold tethering electrode. To the initial layer was added a second layer of mobile phase lipid molecules of 3 mM DOPC. The layers were left to incubate at room temperature for exactly two minutes before a rapid exchange of 3 x 200 µL 100 mM NaCl Tris buffer to induce the formation of a complete tBLM.

Swept frequency (0.1-2000 Hz) electrical impedance spectroscopy was applied at 25 mV peak-to-peak using a Tethapod^{TM} impedance spectrometer (SDx Tethered Membranes Pty Ltd, NSW, Australia). Impedance and phase profiles were fitted to an equivalent circuit consisting of a tethering gold electrode and reservoir region connected in series with a resistor to represent

the impedance of the surrounding electrolyte solution, and a resistor/capacitor representing the lipid bilayer (as previously described).[29] The data were fitted using an adapted Levenberg-Marquardt fitting method incorporated into the TethaQuick[TM] software (SDx Tethered Membranes Pty Ltd, NSW, Australia).

2.5 MTS cell viability assay

MDA-MB-231 cells were seeded in triplicate in clear bottom 96-well plates (5×10^3 cells per well) and incubated overnight. After 24 h the media was removed, and cells were treated with various concentrations of the test compounds in DMSO (final concentration 0.1%) and incubated for 48 h. Cells were then incubated with CellTiter MTS 96® Aqueous MTS Reagent Powder (Promega) and phenazine ethosulfate (Sigma-Aldrich) under dark conditions for 3 h. The absorbance of each well at 490 nm was measured using a Tecan Infinite M1000 Pro plate reader to evelute cell viability according to the manufacturer's recommendation (CellTiter 96® Aqueous One Solution Cell Proliferation Assay, Promega, Wisconsin, USA). MTS IC50 values were defined as the drug concentration that prevented more than 50% of cell growth (relative to the control) and determined using nonlinear regression analysis with Prism 8.4.3 (GraphPad Software, California, USA).

2.6 Seahorse XF analysis

Seahorse XF sensor cartridges were hydrated for 24 h prior to the experiments using Seahorse XF calibrant at 37 °C in a humidified non-CO_2 atmosphere. MDA-MB-231 cells were seeded in XF 24 cell culture microplates (2×10^4 cells per well) and incubated for 24 h in a humidified atmosphere of 5% CO_2. The cells were washed twice with XF Base medium supplemented with 10 mM D-(+)-glucose, 2 mM L-glutamine and 1 mM sodium pyruvate at pH 7.4 prior to the final addition of 450 µL assay medium/well. The cells were incubated at 37

°C in a humidified non-CO$_2$ atmosphere for 1 h. The loaded XF sensor cartridge was placed into a Seahorse XFe24 Analyser and calibrated. Once calibrated, the calibration fluid was replaced with XF 24 cell culture microplates containing cells. Test compounds/DMSO (50 µL) were injected into designated wells and the first set of OCR measurements were recorded. After 3 cycles, oligomycin (1 µM), FCCP (2 µM), and rotenone/Antimycin A (0.5 µM) were successively injected into each well. OCR was measured using a cycling program where 3 measurements were recorded between each injection. Readings for the last of each 3 cycles were used for OCR data analysis. OCR parameters were calculated as follows: post-treatment respiration = Basal OCR – Rotenone/Antimycin A OCR; Maximal respiration = FCCP OCR – Rotenone/Antimycin A OCR; ATP production = post-treatment respiration OCR – Oligomycin OCR.

2.7 JC-1 mitochondrial membrane potential assay

MDA-MB-231 cells were seeded in triplicate in 96-well black/clear bottom plates (1.5 x 10^4 cells per well) and incubated overnight. After 24 h, the media was removed and cells were treated with various concentrations of the test compounds in DMSO (final concentration 0.1%) and incubated for 1 h. Cells were incubated with JC-1 for 20 minutes in media, washed with PBS (2 x 200 µL), and 200 µL of PBS was added to each well. The JC-1 red/green fluorescence ratio was measured using a Tecan Infinite M1000 Pro plate reader to determine red (595/535 nm) and green (535/485 nm) emmision/excitation wavelengths according to the manufacturer's recommendation (JC-1 Mitochondrial Membrane Potential Kit, Cayman Chemical, Michigan, USA).

2.8 Intracellular ATP assay

MDA-MB-231 cells were seeded in triplicate in 96-well black/clear bottom plates (1 x 10^4 cells per well) and incubated overnight. After 24 h the media was removed, and cells were treated with the test compounds in DMSO (final concentration 0.1%) and incubated for the duration of the experiment. Cells were incubated with CellTiter-Glo® in media, mixed for 2 minutes in an orbital shaker, and left at room temperature under dark conditions for 10 minutes, after which luminescence was read using a Tecan Infinite M1000 Pro plate reader to quantify intracellular ATP levels according to the manufacturer's recommendation (CellTiter-Glo® 2.0 Luminescent Cell Viability Assay, Promega, Wisconsin, USA).

2.9 LDH release assay

MDA-MB-231 cells were seeded in triplicate in 96-well black/clear bottom plates (1 x 10^4 cells per well) and incubated overnight. After 24 h the media was removed, and cells were treated with the test compounds in DMSO (final concentration 0.1%) and incubated for 6 h. Aliquots of treatment medium (3 μL) were taken from each well and combined with LDH storage buffer previously prepared according to the manufacturer's instructions (LDH-Glo™ Cytotoxicity Assay, Promega, Wisconsin, USA). The combined solutions were incubated with prepared LDH detection reagent at room temperature under dark conditions for 60 min and luminescence was read using a Tecan M1000 Pro plate reader to quantify levels of extracellular LDH according to the manufacturer's recommendation (LDH-Glo™ Cytotoxicity Assay, Promega, Wisconsin, USA). Values were standardised to cells lysed in cell media containing Triton X-100 (0.2% v/v) and are expressed as a percentage of maximal LDH release (see **Table S1** in Supporting Information).

2.10 DCFDA assay

MDA-MB-231 cells were seeded in triplicate in 96 well black/clear bottom plates (2 x 10^4 cells per well) and incubated overnight. After 24 h the media was removed, and cells were

treated with 100 µL of 20 µM DCFDA solution (prepared in phenol red-free and serum-free DMEM) and incubated for 25 min. Each well was washed with PBS (2 x 200 µL) and 100 µL of phenol red-free DMEM (1% FBS) was added. Cells were treated with various concentrations of the test compounds in DMSO (final concentration 0.1%) and incubated for 10 min. Fluorescence intensity was measured using a Tecan M1000 Pro plate reader to determine emission/excitation wavelengths at 529/495 nm. Fluorescence was continuously monitored and final readings during linear changes were reported with respect to time-matched DMSO-treated control cells.

2.11 Statistical analysis

All data are expressed as means ± SEM of 3 independent experiments (N = 3) unless otherwise specified. Normalised dose-response curves were constructed using GraphPad Prism 8.4.3 to calculate absolute and relative IC_{50} concentrations (see Supporting Information). ATP and LDH release data are expressed as means ± SEM of time-matched DMSO-treated and Triton X-100-treated controls, respectively, and were analysed by two-way ANOVA with Dunnett's multiple comparison test. DCFDA data are expressed as means ± SEM and were analysed by two-way ANOVA with Dunnett's multiple comparison test. Seahorse and tBLM data were normalised to baseline DMSO controls prior to the addition of test compounds.

3.   Results and discussion:

3.1 Design and synthesis of IL library

To understand how the cationic head group affects cytotoxicity of aromatic AmILs, we synthesised a series of ILs with diverse cationic head group structures (see **Table 1**). All AmILs were prepared with *N*-hexadecyl chains and iodide anions so that any changes in cytotoxicity could be attributed to head group properties. The properties of interest were:

- Head group size**:** AmILs with mono- and bicyclic head groups were prepared. Cycles were fused or connected by alkyl groups of different lengths and geometries. The bipyridyl based analogues **4** and **5** were prepared with 2,3'-substitution as 2,2'-, 2,4'- and 4,4'-bipyridyl salts (e.g., paraquat) can induce cytotoxic and mitochondrial effects through redox-associated activity that may cloud the SAR.[30,31]

- Head group lipophilicity: AmILs containing structurally related head groups of differing lipophilicity were prepared (see **Table S1** in Supporting Information for calculated Log P values of each head group) by direct substitution of head group carbon atoms for nitrogen atoms, for example pyridine to pyrimidine.

- Head group charge**:** assessed by comparison of structurally related ILs bearing either mono- or dicationic head groups.

Compounds **1-4** and **6-15** were synthesised using single-step Menshutkin reactions of 1-iodohexadecane and the appropriate heterocycles (see **Scheme S1** in Supporting Information). For reactions involving heterocycles with multiple nitrogen atoms, quaternisation occurred at the least sterically hindered and/or most basic nitrogen atoms, as steric effects impose greater limitations on quaternisation reaction rates.[32,33] The dicationic IL **5** was prepared from **4** by a Menshutkin reaction with iodomethane (see **Scheme S2** in Supporting Information). ILs **13** and **14** were also prepared in two synthetic steps. Firstly, amino-nitrogen atoms in heterocycles **16** and **17** were methylated with iodomethane to afford **18** and **19**, which were alkylated at the imino-nitrogen units with 1-iodohexadecane to yield **13** and **14** (see **Scheme S3** in Supporting Information). Full synthetic procedures and characterisation data can be found in the Supporting Information.

*3.2 Effects of AmILs **1-14** on cell viability*

We performed MTS assays to examine the effects of **1-14** on the viability of human MDA-MB-231 breast cancer cells. Dose-response curves were constructed (see **Figure S1** in Supporting Information) and used to calculate IC_{50} concentrations, which are shown in **Table 1**. ILs **1-14** were found to reduce MDA-MB-231 cell viability with IC_{50} concentrations ranging from ~ 2 – 25 μM, except for **7** which had no effect cell viability when tested at its solubility of 100 μM in cell media. To confirm that the MTS data reflected reductions in cell viability, phase-contrast images of MDA-MB-231 cells treated with **1-14** above their MTS IC_{50} concentrations were taken (see **Figure S3** in Supporting Information). These images revealed that MTS active compounds reduced the number of viable cells and altered their morphology at concentrations above their IC_{50} concentrations, while the inactive **7** (50 μM) lacked these effects.

The MTS data indicates that increased head group lipophilicity promotes cytotoxicity within structurally-related AmILs. This effect is demonstrated by pairwise comparison of the IC_{50} concentrations of pyrimidyl-based IL **2** and pyridyl-based **1** (head group Log P values = -0.21 and 0.70, respectively), and analogues **4** to **3** (head group Log P values = 1.77 and 2.49, respectively). In both cases the inclusion of an additional nitrogen atom into the head group by direct substitution of a carbon atom, which lowers head group Log P by ~ 0.8 units, produced 3- to 5-fold decreases in cytotoxicity. The impact of lipophilicity was overall quite modest and could be overcome by other structural features. For example, the IC_{50} concentration of methyl-imidazolium based AmIL **10** (head group Log P = -0.18) was almost half that of AmIL **8** (head group Log P = 1.56).

Comparison of AmILs bearing common quaternised heterocycles indicates that increasing the size of the head group through addition of a phenyl ring increases cytotoxicity. For example, substitution of the pyridinium-based AmIL **1** and imidazolium-based AmIL **10** with phenyl groups (to give **3** and **11**, respectively) resulted with 2- to 4-fold increases in

cytotoxicity. Fusion of an additional benzene ring to the head group increased activity, as shown by the benzimidazolium-based analogue **12**, which is 4-fold more potent than its imidazolium-based counterpart **10**. Similarly, benzimidazolium-based IL **14** is more cytotoxic than **13**, although the difference in IC_{50} concentrations between these two AmILs is modest.

While substitution and/or fusion of phenyl groups to the head group increased activity, addition of a pyridine ring had moderate effects on potency. For example, the bipyridyl-based AmIL **4** was equipotent to the pyridinium-based AmIL **1**, and the pyridyl-substituted analogue **13** had an IC_{50} value of 8.5 ± 1.6 µM, which is comparable the IC_{50} concentration of its imidazolium-based counterpart **10** (IC_{50}: 13.4 ± 0.8 µM). This finding is unexpected as extension with an additional pyridine ring increases both head group size and lipophilicity. Addition of a non-aromatic heterocycle appeared to lower cytotoxicity, as shown by the comparison of **8** to **1.**

Included in this test set were two dicationic AmILs. **7**, a dicationic analogue of **6** that carries two hexadecyl chains in the head group, was the only compound that did not reduce cell viability at concentrations up to 100 µM. **5** is a dicationic analogue of **4** substituted with an additional methyl group. **4** and **5** displayed equipotent activity and reduced cell viability with IC_{50} concentrations of 8.3 ± 0.9 µM and 8.0 ± 0.1 µM, respectively. These data indicate that dicationic AmILs are not more cytotoxic than their cationic counterparts, and inclusion of two long alkyl groups significantly lowers cytotoxicity.

Collectively, the SAR insights add new information regarding the influence of cationic head group structure on IL cytotoxicity. Excluding the dicationic AmILs, the IC_{50} concentrations ranged from approximately 2 – 25 µM, which shows that head group structure has a modest impact on the cytotoxicity of AmILs in comparison to *N*-alkyl chain length. For example, extending the *N*-alkyl chain of methylimidazolium-based AmILs from 4 to 10 carbons increases cytotoxicity towards HeLa cells approximately ~ 160-fold.[15] Decreases in

activity that occurred when carbon atoms in the head group were substituted with nitrogen atoms suggests that lipophilic head groups promote cytotoxicity. This is consistent with previous reports which have shown that non-aromatic ILs are less cytotoxic than aromatic analogues due to the relatively polar nature of non-aromatic head groups.[15,22,24-26] Prior to this study there was some evidence to suggest that larger head groups promote AmIL cytotoxicity,[16] and the data presented here is consistent with this finding, as shown by gains in activity that resulted from the addition of a phenyl ring to the head group, either by substitution or fusion. In contrast, when head group size was increased by addition of a pyridine ring only moderate increases in activity were observed. This may be attributed to the relatively polar nature of the pyridyl ring in comparison to a phenyl ring, where the increase in head group size is offset by changes in headgroup lipophilicity. Consistent with previously reported data,[11,34] we found that dicationic AmILs substituted with an additional small alkyl groups (methyl) are equipotent to their monocationic counterparts. In contrast, additional of a second long alkyl chain produced a dicationic AmIL that lacked cytotoxicity at concentrations up to 100 μM.

Table 1. Chemical structures and absolute MTS IC$_{50}$ concentrations of ILs **1-14** measured in human MDA-MB-231 breast cancer cells.[a]

Cmpd	Structure	MTS IC$_{50}$ [μM]	Cmpd	Structure	MTS IC$_{50}$ [μM]
1		7.7 ± 0.3	**8**		22.1 ± 2.9
2		24.4 ± 1.7	**9**		11.0 ± 1.5
3		1.6 ± 0.3	**10**		13.4 ± 0.8
4		8.0 ± 0.1	**11**		7.0 ± 0.4
5		8.3 ± 0.9	**12**		3.0 ± 0.9
6		22.7 ± 1.2	**13**		8.5 ± 1.6
7		>100[b]	**14**		5.1 ± 0.5

[a] Cell viability measured using the MTS assay after 48 h treatment

[b] No effect on cell viability detected at the maximum tested concentration of 100 μM

*3.3 Effects of AmILs **1** and **2** on phospholipid bilayer conductance and mitochondrial function*

Next we conducted mechanistic studies to understand the cellular targets and pathways associated with the cytotoxicity of pyridinium-based IL **1** and pyrimidinium-based **2.** Previous studies have shown that AmILs exert cytotoxicity by disrupting cellular membranes and/or inducing mitochondrial dysfunction.[15,19,35-39] Mitochondria are sites of important cellular processes including regulation of reactive oxygen species (ROS) and synthesis of adenosine triphosphate (ATP) by oxidative phosphorylation (OXPHOS).[40] During OXPHOS nutrient oxidation is used by the electron transport chain (ETC) to pump protons across the inner mitochondrial membrane (IMM), and the resulting proton gradient establishes a transmembrane potential ($\Delta\Psi_m$) across the IMM. $\Delta\Psi_m$ drives protons through ATP-synthase to catalyse ATP production. We recently showed that AmILs accumulate in the IMM in response to $\Delta\Psi_m$ and permeabilise the membrane, subsequently collapsing the proton gradient that sustains $\Delta\Psi_m$, inhibiting ATP production, and increasing cellular ROS production.[15] To determine if AmILs in this study exerted similar effects, pyridinium-based IL **1** and pyrimidinium-based **2** were selected for mechanistic studies.

We first assessed the capacity of **1** and **2** to permeabilise phospholipid bilayers using tethered lipid bilayer membranes (tBLMs). The experimental setup consists of a lipid bilayer anchored between gold electrodes, where the inner leaflet is interspaced with thiol-based spacer molecules that provide scaffolding and tethered the bilayer to one gold electrode.[28] Permeabilisation of the membrane in response to the addition of a membrane-disrupting agent is detected as a change in ionic conductance across the membrane and can be measured by electrical impedance spectroscopy. For these studies, tBLMs were assembled with 1,2-dioleoyl-*sn*-glycero-3-phosphocholine (DOPC) as it is the most abundant phospholipid in the IMMs of mammalian cells.[41] As shown in **Figure 2**, addition of the pyridinium-based **1** produced a rapid increase in membrane ionic conductance, which reached approximately 700%

of the control several minutes after treatment. The less cytotoxic AmIL **2** also increased

membrane conductance, however to a lesser extent than that produced by **1**. That AmIL **2** had

less impact on membrane permeability than **1** is consistent with previous studies which have

shown that AmILs with polar headgroups head groups have reduced capacity to disrupt lipid

bilayers.[16] The difference arises because the headgroup affects the interaction of AmILs with

membranes. AmILs compromise membrane structural integrity by inserting into the bilayer

with the *N*-alkyl tail extending into the hydrophobic core of the bilayer and the headgroup at

the water-lipid interface.[36,37] AmILs with relatively large and/or lipophilic headgroups induce

disorder in chain dynamics and lipid packing by changing the orientation of the phosphocholine

groups in POPC bilayers, which leads to permeabilisation of the membrane.[16] AmILs with

relatively polar headgroups have lower membrane affinity, and the polar nature of the

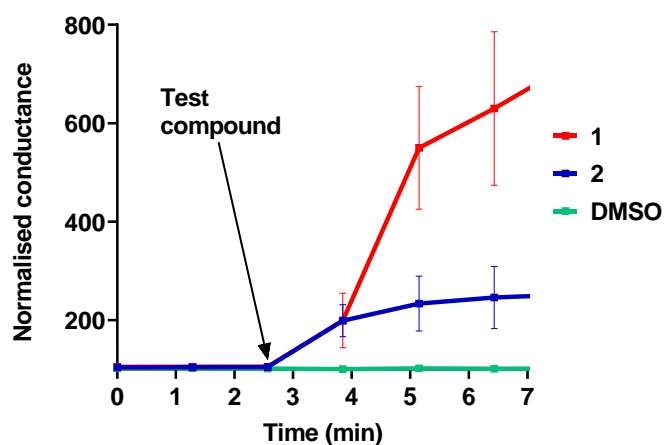headgroup minimises structural perturbations and impacts on lipid orientation.[16]

Figure 2. The effects of **1** and **2** (10 µM) on the ionic conductance of DOPC lipid
bilayers tethered to gold electrodes as measured by electrical impedance spectroscopy. Data
were normalised to a baseline control and represent the mean ± SEM from 3 independent
experiments.

We next assessed the effects of **1** and **2** on mitochondrial function in MDA-MB-231 cells.

In these assays, cells were treated with the AmILs at their MTS IC_{50} concentrations for short

time periods to observe early cellular events likely associated with their cytotoxic effects. The Seahorse Mito Stress test is used to detect changes in mitochondrial function by measuring cellular oxygen consumption rate (OCR) and extracellular acidification rate (ECAR), which are proportional to the rates of OXPHOS and glycolysis, respectively. It was anticipated that AmIL-mediated permeabilisation of the IMM would collapse $\Delta\Psi_m$, inhibit ATP production by OXPHOS and shift the cells to glycolysis to meet cellular ATP demands. As shown in **Figures 3A** and **3C**, the addition of **1** and **2** to MDA-MB-231 cells produced a rapid decrease in cellular OCR relative to DMSO-treated cells, and an associated increase in ECAR (see **Figure 3B**), which is proportional to glycolytic activity. Consistent with previous findings,[15,19] these data suggest that **1** and **2** inhibit OXPHOS, and in response treated cells shift metabolic activity from OXPHOS to glycolysis to produce ATP. Maximal respiration, measured after the addition of FCCP, reflects the functional status of the ETC post-treatment with the AmILs. **1** and **2** reduced maximal respiration relative to control (see **Figure 3C**), which suggests that these ILs induce mitochondrial dysfunction.[42] Consistent with the MTS and tBLM data, pyridinium-based AmIL **1** reduced maximal respiration to a greater extent than **2**. In cells treated with **1** and **2**, maximal respiratory capacities were below post-treatment levels, indicating that these cells had diminished spare respiratory capacity. Spare respiratory capacity is a measure of the ability of a cell to respond to bioenergetic demands during stress, and low capacities indicate an inability to meet cellular ATP demand.[42] ATP production is measured as the decrease in OCR following the addition of oligomycin and represents the portion of mitochondrial produced ATP. Both **1** and **2** (**Figure 3C**) decreased OCR associated with ATP production. Taken together, these data suggest that **1** and **2** inhibit OXPHOS in MDA-MB-231 cells at their MTS IC_{50} concentrations and induce mitochondrial dysfunction, consistent with permeabilisation of the IMM.
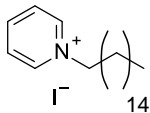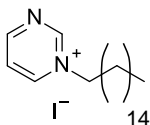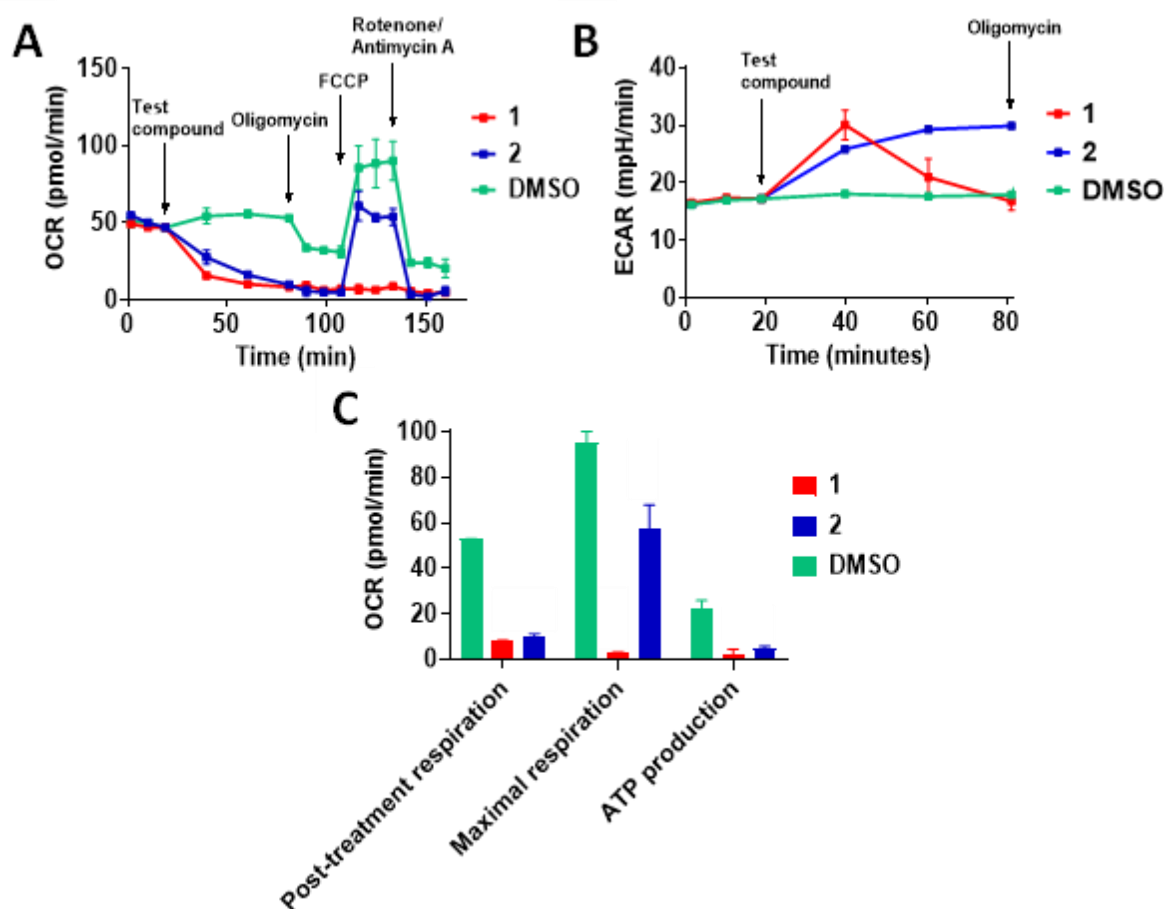
Figure 3. Effects of **1** and **2** on mitochondrial function in MDA-MB-231 cells measured using a Seahorse XFe24 Analyser. **A** Oxygen consumption rates of cells treated with sequential additions of the AmILs at their MTS IC_{50} concentrations, followed by oligomycin (1 µM), FCCP (2 µM), and rotenone/Antimycin A (1 µM). **B** ECAR of MDA-MB-231 cells following treatment with **1** and **2** at their MTS IC_{50} concentrations. **C** OCR parameters associated with post-treatment respiration, maximal respiration, and ATP production in MDA-MB-231 cells following treatment of **1** and **2**. Data were normalised to a baseline control and represent the mean of 2 separate wells from the same experiment.

To evaluate the capacity of **1** and **2** to reduce $\Delta\Psi_m$ in MDA-MB-231 cell mitochondria, we performed JC-1 assays. JC-1 is a redox-active dye that accumulates in the mitochondrial matrix of polarised mitochondria with high $\Delta\Psi_m$, forming aggregates that fluoresce red. In

response to the collapse of the proton gradient and loss of $\Delta\Psi_m$, JC-1 diffuses into the cytosol where it dissociates to monomers that fluoresce green. Ratio of JC-1 red/green fluorescence can therefore be used to measure $\Delta\Psi_m$, and we determined JC-1 IC_{50} concentrations as concentrations required to shift the red/green fluorescence ratio by 50% (see **Figure S2** in Supporting Information). The maximum effect (E_{max}) values represent the maximum shifts in the red/green fluorescence ratio produced by each AmIL (see **Figure S2** in Supporting Information for JC-1 dose-response curves). Short treatments (1 hour) were used to distinguish direct effects of the ILs on the IMM from dissipation of $\Delta\Psi_m$ that can occur from apoptotic cell death. Both AmILs shifted JC-1 red/green fluorescence ratio with IC_{50} concentrations that were comparable to their MTS IC_{50} concentrations (see **Table 2**). In addition to their potencies, the E_{max} values of each AmIL in JC-1 assays also reflected their activities in MTS assays as the E_{max} of the more cytotoxic AmIL **1** was lower that than of **2**. Together, these data suggest that **1** can collapse the proton gradient across the IMM with greater efficiency and magnitude than **2**, and that the capacity of each AmIL to reduce $\Delta\Psi_m$ is associated with their cytotoxicity.

Table 2. Relative IC_{50} concentrations and maximum effect (E_{max}) values of **1** and **2** (1 hour treatment) measured in JC-1 assays.

Cmpd	Structure	JC-1 IC_{50} [μM]	E_{max}
1		7.9 ± 0.4	$24.9 \pm 2.5\%$
2		28.7 ± 3.5	$57.3 \pm 2.9\%$

Collapse of $\Delta\Psi_m$ is expected to lead to inhibition of ATP synthesis by OXPHOS, so we measured intracellular ATP levels in MDA-MB-231 cells treated with **1** and **2** for 2, 4 and 6 hours. As shown in **Figure 4A**, **1** and **2** reduced ATP levels to $73 \pm 4.2\%$ and $54 \pm 3.5\%$ of

DMSO-treated control cells after 6 hours, respectively. To confirm that observed changes in ATP levels were not the result of decreased cell viability, we performed lactate dehydrogenase (LDH) release assays as a marker of cell death.[43] These assays showed that **1** and **2** did not induce LDH release relative to DMSO-treated cells for up to 6 hours (see **Table S2** in Supporting Information), which supports the conclusion that **1** and **2** inhibit intracellular ATP
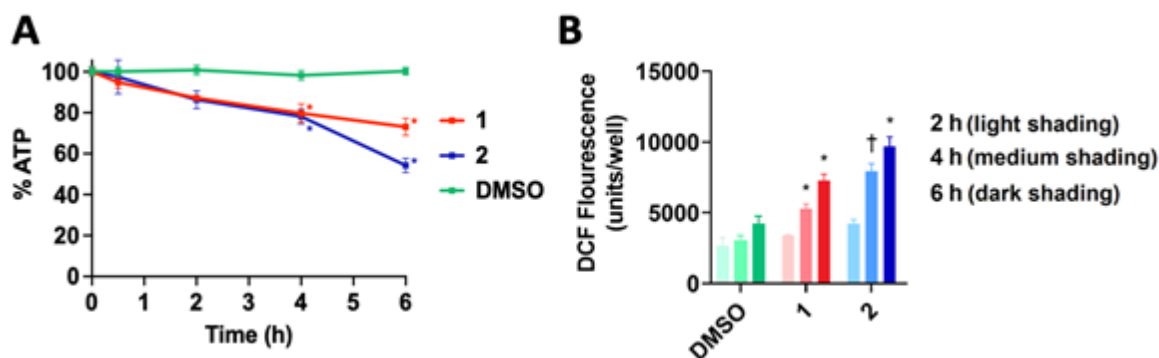
production.

Figure 4. A Quantification of total intracellular ATP content in MDA-MB-231 cells following treatment with **1** and **2** at their JC-1 IC_{50} concentrations. Data represent the mean $\pm$ SEM of time-matched DMSO controls from 3 independent experiments performed in triplicate. Significantly different from DMSO control: (*) $p < 0.05$. **B** ROS production in MDA-MB-231 cells following treatment with **1** and **2** at their JC-1 IC_{50} concentrations. Data represent the mean $\pm$ SEM from 3 independent experiments performed in triplicate. Significantly different from DMSO control: (*) $p < 0.05$, ($\dagger$) $p < 0.01$.

We next assessed the capacity of **1** and **2** to induce ROS formation in MDA-MB-231 cells using the DCFDA assay. In this assay cells were treated with **1** and **2** at their JC-1 IC_{50} concentrations. Mitochondria are important sites of ROS production and several studies have shown that AmILs can induce ROS production.[15,19,20] The precise mechanism is unknown, however it has been suggested that increased ROS may result from the interactions of the AmIL with the ETC[19] or as a consequence of permeabilisation of the IMM.[44] As shown in **Figure 4B**, **1** and **2** produced significant increases in cellular ROS levels after 4 hours of treatment time and reached ~ 2-fold of control after 6-hour treatment. That the AmILs increased ROS

formation is significant because excessive intracellular ROS levels are known to trigger cell death through oxidative damage that can cause mutations in both nuclear and mitochondrial DNA.[40]

Taken together, the mechanistic studies indicate that the AmILs permeabilise the IMM, which results in a series of mitochondrial effects including increased ROS production that are associated with cell death. That the IMM is the target of cytotoxic AmILs is also consistent with the observed SAR as the headgroup properties that promote cytotoxicity (increased size and lipophilicity) are also associated with greater capacity to disrupt lipid bilayers such as the IMM.

4.   Conclusions:

In summary, the data presented here shows that the structure of the cationic head group in AmILs does impact cytotoxicity, albeit to a lesser than variation of the *N*-alkyl chain. Increasing the size and/or lipophilicity of the headgroup through substitution and/or fusion with phenyl rings increased AmIL cytotoxicity, whereas increasing headgroup polarity via inclusion of additional nitrogen atoms lowered cytotoxicity. Expansion of headgroup with additional heterocycles had a minor impact on activity. Mechanistic studies indicated that the AmILs permeabilise the IMM and induce mitochondrial dysfunction including depolarisation of the IMM, inhibition of ATP synthesis and increases ROS production. These effects are consistent with the observed SAR as increased head group size and lipophilicity may promote the capacity of the AmILs to partition into and disrupt the IMM.

22

References:

1. Egorova K., Gordeev E., Ananikov V. (2017). "Biological activity of Ionic Liquids and Their Application in Pharmaceutics and Medicine" *Chemical Reviews* **117** (10): 7132-7189.

2. Goossens K., Lava K., Bielawski C., Binnemans K. (2016). "Ionic Liquid Crystals: Versatile Materials" *Chemical Reviews* **116** (8): 4643-4807.

3. Patel D. & Lee J. (2012). "Applications of Ionic Liquids" *Chemical Record* **12** (3): 329-355.

4. Amde M., Liu J., Pang L. (2015). "Environmental Application, Fate, Effects, and Concerns of Ionic Liquids: A Review" *Environmental Science & Technology* **49** (21): 12611-12627.

5. Bernot R., Kennedy E., Lamberti G. (2005). "Effects of ionic liquids on the survival, movement, and feeding behaviour of the freshwater snail, *Physa acuta*" *Environmental Toxicology and Chemistry* **24** (7): 1759-1765.

6. Luis P., Garea A., Irabien A. (2010). "Quantitative structure-activity relationships (QSARs) to estimate ionic liquids ecotoxicity EC_{50} (*Vibrio fischeri*)" *Journal of Molecular Lipids* **152** (1-3): 28-33.

7. McLaughlin M., Earle M., Gîlea M., Gilmore B., Gorman S., Seddon K. (2011). "Cytotoxicity of 1-alkylquinolinium bromide ionic liquids in murine NIH 3T3 cells" *Green Chemistry* **13** (10): 2794-2800.

8. Musiał M., Zorębski E., Malarz K., Kuczak M., Mrozek-Wilczkiewicz A., Jacquemin J., Dzida M. (2021). "Cytotoxicity of Ionic Liquids on Normal Human Dermal Fibroblasts in the Context of Their Present and Future Applications" *ACS Sustainable Chemistry & Engineering* **9** (22): 7649-7657.

9. Oskarsson A. & Wright M. (2019). "Ionic Liquids: New Emerging Pollutants, Similarities with Perfluorinated Alkyl Substances (PFASs)" *Environmental Science & Technology* **53** (18): 10539-10541.

10. Fang Z., Zheng X., Li L., Qi J., Wu W., Lu Y. (2022). "Ionic Liquids: Emerging Antimicrobial Agents" *Pharmaceutical Research* **39** (10): 2391-2404.

11. Pérez S., Montalbán M., Carissimi G., Licence P., Víllora G. (2020). "*In vitro* cytotoxicity assessment of monocationic and dicationic pyridinium-based ionic liquids on HeLa, MCF-7, BGM and EA.hy926 cell lines" *Journal of Hazardous Materials* **385**: 1-9.

12. Li X., Ma J., Wang J. (2015). "Cytotoxicity, oxidative stress, and apoptosis in HepG2 cells induced by ionic liquid 1-methyl-3-octylimidazolium bromide" *Ecotoxicology and Environmental Safety* **120**: 342-348.

13. Dzhemileva U., D'yakonov V., Seitkalieva M., Kulikovskaya N., Egorova K. Ananikov V. (2021). "A large-scale study of ionic liquids employed in chemistry and energy research to reveal cytotoxicity mechanisms and to develop a safe design guide" *Green Chemistry* **23** (17): 6414-6643.

14. Stolte S., Arning J., Bottin-Webber U., Matzke M., Stock F., Thiele K., Uerdingen M., Welz-Biermann, Jastorff B., Ranke J. (2006). "Anion effects on the cytotoxicity of ionic liquids" *Green Chemistry* **8**: 621-629.

15. Duman M.N., Angeloski A., Johnson M., Rawling T. (2023). "Aromatic long chain cations of amphiphilic ionic liquids permeabilise the mitochondrial inner membrane and induce mitochondrial dysfunction at cytotoxic concentrations" *Green Chemistry* **25**: 6067-6076.

16. Kaur N., Fischer M., Kumar S., Gahlay G. K., Scheidt H., Mithu V. S., (2021). "Role of cationic head-group in cytotoxicity of ionic liquids: Probing changes in bilayer

architecture using solid-state NMR spectroscopy" *Journal of Colloid and Interface Science* **581**: 954-963.

17. Fernandes M., Carvalho E., Correia D., Esperança J., Padrão J., Ivanova K., Hoyo J., Tzanov T., Lanceros-Mendez S. (2022). "Ionic Liquids as Biocompatible Antimicrobial Agents: A Case Study on Structure-Related Bioactivity on *Escherichia coli*" *ACS Applied Bio Materials* **5** (11): 5181-5189.

18. Türkmen H., Ceyhan N., Yavaşoğlu Ü.K., Özdemir G., Çetinkaya B. (2011). "Synthesis and antimicrobial activities of hexahydroimidazo[1,5-*a*]pyridinium bromides with varying benzyl substituents" *European Journal of Medicinal Chemistry* **46** (7): 2895-2900.

19. Abdelghany T., Lietch A., Nevjestic A., Ibrahim I., Miwa S., Wilson C., Heutz S., Wright M. (2020). "Emerging risk from "environmentally friendly" solvents: Interaction of methylimidazolium ionic liquids with the mitochondrial electron transport chain is a key initiation event in their mammalian toxicity" *Food and Chemical Toxicology* **145**: 1-14.

20. Ma J. & Li X. (2018). "Insight into the negative impact of ionic liquid: A cytotoxicity mechanism of 1-methyl-3-octylimidazolium bromide" *Environmental Pollution* **285**: 1337-1345.

21. Yoo B., Jing B., Jones S., Lamberti G., Zhu Y., Shah J., Maginn E. (2016). "Molecular mechanisms of ionic liquid cytotoxicity probed by an integrated experimental and computational approach" *Scientific Reports* **6** (1): 1-7.

22. Farahani S., Sohrabi M., Ghasemi J. (2018). "A detailed structural study of cytotoxicity effect of ionic liquids on the leukemia rat cell line IPC-81 by three dimensional quantitative structure toxicity relationship" *Ecotoxicology and Environmental Safety* **158**: 256-265.

23. Frade R., Matias A., Branco L., Alfonso C., Duarte C. (2007). "Effect of ionic liquids on human colon cancer carcinoma HT-29 and CaCo-2 cell lines" *Green Chemistry* **9**: 873-877.

24. Kumar R., Papaiconomou N., Lee J., Salimen J., Clark D., Prausnitz J. (2008). "*In Vitro* Cytotoxicities of Ionic Liquids: Effect of Cation Rings, Functional Groups, and Anions" *Environmental Toxicology* **24** (4): 388-395.

25. Frade R., Rosatella A., Marques C., Branco L., Kulkarni P., Mateus N., Afonso C., Duarte C. (2009). "Toxicological evaluation on human colon carcinoma cell line (CaCo-2) of ionic liquids based on imidazolium, guanidinium, ammonium, phosphonium, pyridinium and pyrrolidinium cations" *Green Chemistry* **11** (10): 1660-1665.

26. Stolte S., Arning J., Bottin-Weber U., Müller A., Pitner W.R., Welz-Biermann U., Jastorff B., Ranke J. (2007). "Effects of different head groups and functionalised side chains on the cytotoxicity of ionic liquids" *Green Chemistry* **9**: 760-767.

27. Pauli G., Chen S.N., Simmler C., Lankin D., Gödecke T., Jaki B., Friesen B.F., McAlpine J., Napolitano J. (2014) "Importance of Purity Evaluation and the Potential of Quantitative ^{1}H NMR as a Purity Assay" *Journal of Medicinal Chemistry* **58** (22): 9220-9231.

28. Cranfield C., Carne, S., Martinac B., Cornell B. (2015). "The Assembly and Use of Tethered Bilayer Lipid Membranes (tBLMs)" *Methods in Molecular Biology* **1232**: 45-53.

29. Cranfield C., Henriques S., Martinac B., Duckworth P., Craik D., Cornell B. (2017). "Kalata B1 and Kalata B2 Have a Surfactant-Like Activity in Phosphatidylethanolamine-Containing Lipid Membranes" *Langmuir* **33** (26): 6630-6637.

30. Gao L., Yuan H., Xu E., Liu J. (2020). "Toxicology of paraquat and pharmacology of the protective effect of 5-hydroxy-1-methylhydantoin on lung injury caused by paraquat based on metabolomics" *Scientific Reports* **10** (1): 1-16.

31. Homer R. F., Mees G. C., Tomlinson T. E. (1960). "Mode of action of dipyridyl quaternary salts as herbicides" *Journal of the Science of Food and Agriculture* **11** (6): 309-315.

32. Deady L. & Stillman D. (1976). "Steric Effects in Quaternizations. Alkylation of Pyridine, Thiazole, Isothiazole and Some Benzologues with Methyl, Ethyl and Isopropyl Iodides" *Australian Journal of Chemistry* **29** (8): 1745-1748.

33. Brown H. & Cahn A. (1955). "Steric Effects in Displacement Reactions. II. The Rates of Reaction of Alkyl Iodides with the Monoalkylpyridines. Steric Strain in the Activated Complex" *Journal of the American Chemical Society* **77** (7): 1715-1723.

34. Gindri I., Siddiqui D., Bhardwaj P., Rodriguez L., Palmer K., Frizzo C., Martins M., Rodrigues D. (2020). "Dicationic imidazolium-based ionic liquids: a new strategy for non-toxic and antimicrobial materials" *RSC Advances* **4** (17): 62594-62602.

35. Galluzzi M., Schulte C., Milani P., Podestà A. (2018). "Imidazolium-Based Ionic Liquids Affect Morphology and Rigidity of Living Cells: An Atomic Force Microscopy Study" *Langmuir* **34** (41): 12452-12462.

36. Kumari P., Pillai V., Rodriguez B., Prencipe M., Benedetto A. (2020). "Sub-Toxic Concentrations of Ionic Liquids Enhance Cell Migration by Reducing the Elasticity of Cellular Lipid Membrane" *The Journal of Physical Chemistry Letters* **11** (17): 7327-7333.

37. Gal N., Malferrari D., Kolusheva S., Galletti P., Tagliavini E., Jelinek R. (2012). "Membrane interactions of ionic liquids: Possible determinants of biological activity and toxicity" *Biochimica et Biophysica Acta* **1818** (12): 2967-2974.

38. Hu L., Xiong Q., Shi W., Huang G., Liu Y., Ying G. (2021). "New insight into the negative impact of imidazolium-based ionic liquid [C_{10}mim]Cl on HeLa cells: From membrane damage to biochemical alterations" *Ecotoxicology and Environmental Safety* **208**: 1-12.

39. Ma J. & Li X. (2018). "Insight into the negative impact of ionic liquid: A cytotoxicity mechanism of 1-methyl-3-octylimidazolium bromide" *Environmental Pollution* **285**: 1337-1345.

40. Milane L., Trivedi M., Singh A., Talekar M., Amiji M. (2015). "Mitochondrial biology, targets, and drug delivery" *Journal of Controlled Release* **207**: 40-58.

41. Horvath S.E. & Daum G. (2013). "Lipids of mitochondria" *Progress in Lipid Research* **52** (4): 590-614.

42. Brand M. & Nicholls D. (2011). "Assessing mitochondrial dysfunction in cells" *Biochemical Journal* **435** (2): 297-312.

43. Legrand C., Bour J.M., Jacob C., Capiaumont J., Martial A., Marc A., Wudtke M., Kretzmer G., Demangel C., Duval D., Hache J. (1992). "Lactate dehydrogenase (LDH) activity of the number of dead cells in the medium of cultured eukaryotic cells as marker of the number of dead cells in medium [corrected]" *Journal of Biotechnology* **25** (3): 231-243.

44. Korge P., John S., Calmettes G., Weiss J. (2017). "Reactive oxygen species production induced by pore opening in cardiac mitochondria: The role of complex II" *The Journal of Biological Chemistry* **292** (4): 9896-9905.